Surface Chemistry

DOI: 10.1002/ange.200600692

Manganese Oxide Nanoparticles Electrodeposited on Platinum Are Superior to Platinum for Oxygen Reduction**

*Mohamed S. El-Deab and Takeo Ohsaka**

A four-electron reduction of molecular oxygen to water at a reasonably low overpotential is the ultimate goal of many investigations. This reaction plays a vital role in electrochemical energy-conversion systems in metal–air batteries and fuel cells. Several attempts have been made at the development of efficient electrocatalysts.[1–18] These include the use of gold-nanoparticle-based electocatalysts which have tunable size and crystallographic orientation.[19–25] The combined use of manganese oxide and cobalt hexadecafluoro or octacyano phthalocyanine has been proposed as novel electrocatalyst for the oxygen-reduction reaction (ORR).[26,27]

Platinum as an electrocatalyst for the ORR is superior to many of the previously investigated electrocatalysts as it supports a direct four-electron reduction of O_2 at relatively low overpotentials. However, the Pt surface suffers from the rapid formation of oxides (especially when used in alkaline media), which causes a gradual decrease of the electrocatalytic performance towards the ORR.[28]

Surface oxides and some specifically adsorbed species at the Pt electrode surface impede the parallel adsorption mode of molecular oxygen, which is a prerequisite for the direct four-electron reduction; the overall reaction is retarded and consequently an appreciable amount of the two-electron reduction product of O_2, hydrogen peroxide, is produced.[3,7,29]

Recent studies show that alloying Pt with Fe results in significant enhancement of the electrocatalytic ability towards the ORR owing to the sharing of the empty d orbital of each Fe center (an electronic factor).[30] In contrast, the enhanced electrocatalysis of Pt upon alloying with Cr, Co, or Ni originates from one or a combination of the following two reasons: 1) the shrinking of the Pt–Pt interatomic distance brought about by alloying (geometric factor);[29,31] 2) retardation of the poisoning of the Pt electrode surface by inhibiting the formation of adsorbed OH species.[6]

Herein we demonstrate an alternative way of modifying a Pt surface. The Pt electrode surface was modified by the electrodeposition of manganese oxide nanoparticles (nano-MnOx), which was done with the expectation of obtaining a durable electrode with high electrocatalytic activity towards the ORR.

Manganese oxide has been widely used as the main constituent material of air batteries owing to its economical and environmental advantages[32,33] in addition to its catalytic activity for oxygen reduction.[28,34,35] Furthermore, this material exhibits a high efficiency towards the catalytic disproportionation of hydrogen peroxide generated at the surface of a Pt electrode (albeit the hydrogen peroxide formation is very slight).

Figure 1a shows a typical scanning electron microscope (SEM) image obtained for the nano-MnOx/Pt electrode. The MnOx is deposited with a porous texture composed of intersected nanorods (average width of about 20 nm) onto the Pt electrode. This porous texture homogeneously covers the entire surface of the electrode, which enables easy access of the solution species to the underlying Pt substrate through channels across the MnOx nanotexture. Transmission electron microscope (TEM) imaging of the MnOx electrodeposited onto Pt mesh (Figure 1b) indicates that the MnOx forms nanorods with an aspect ratio of about 45. The rate of the propagation of the MnOx crystal exceeds the nucleation rate

[*] Prof. Dr. T. Ohsaka
Department of Electronic Chemistry
Tokyo Institute of Technology
4259 Nagatsuta, Midori-ku, Yokohama 226-8502 (Japan)
Fax: (+81) 45-924-5489
E-mail: ohsaka@echem.titech.ac.jp
Homepage: http://www.echem.titech.ac.jp/~ohsaka/ohsaka.html
Dr. M. S. El-Deab
Department of Chemistry
Faculty of Science
Cairo University, Cairo (Egypt)
E-mail: msaada68@yahoo.com

[**] Financial support by New Energy and Industrial Technology Development Organization (NEDO), Japan is greatly acknowledged.

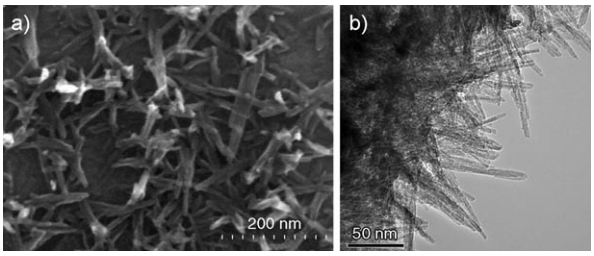

Figure 1. a) SEM image of the nano-MnOx/Pt electrode and b) TEM image of the nano-MnOx/Pt mesh. MnOx nanoparticles were electrodeposited on the Pt electrode or Pt mesh (2000 mesh-grade) from an aqueous solution of Na_2SO_4 (0.1 M) containing $Mn(CH_3COO)_2$ (0.1 M) by applying 25 potential cycles between 0 and 0.4 V versus Ag/AgCl/KCl(sat) at 20 $mV s^{-1}$.[36]

and thus the formation of the nanorods with a high aspect ratio predominates.[37]

Figure 2 shows typical X-ray diffraction (XRD) patterns of Pt substrates loaded with different amounts of nano-MnOx

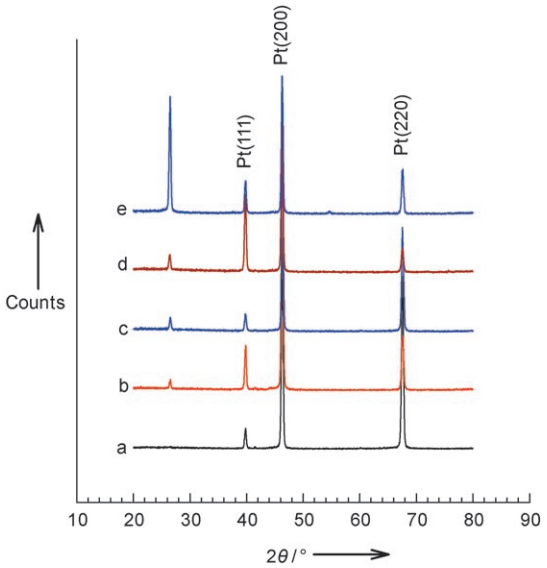

Figure 2. XRD patterns for a) bare Pt, and b–e) nano-MnOx/Pt electrodes. The nano-MnOx/Pt electrodes were prepared in the same way as that described in the caption of Figure 1 with b) 5, c) 25, d) 50, e) 100 potential cycles, respectively.

(patterns b–e) and that of the unloaded Pt substrate (pattern a). The XRD patterns reveal that MnOx is electrodeposited in a crystalline phase giving rise to a sharp peak at a 2θ value of around 26.5°. This peak emerges as MnOx is electrodeposited onto the Pt substrate and corresponds to the $(11\bar{1})$ crystallographic plane of the manganite phase (manganese oxide hydroxide, MnOOH)[38,39].

Steady-state hydrodynamic voltammetry with a rotating ring–disk electrode (RRDE) has long been used to evaluate the electrocatalytic activity of several electrocatalysts towards the ORR.[5–9,19–21,40] Figure 3 shows hydrodynamic voltammograms recorded at 200 rpm for the ORR at a bare Pt disk (curve a; I_D is disk current) and nano-MnOx/Pt disks (curves b and c) with Pt ring electrodes in O_2-saturated KOH solution (0.1 M). The Pt ring was potentiostated at +0.5 V. The top curves (a′–c′) represent the corresponding Pt ring currents (I_R) arising from the oxidation of hydrogen peroxide, HO_2^-, generated at the individual disk electrodes. The ORR current begins to flow at potentials of about +0.025 and +0.05 V (vs. Ag/AgCl) at the nano-MnOx/Pt electrodes prepared by applying 5 (curve b) and 25 (curve c) potential cycles. These potentials are positive by 55 mV (curve b) and 80 mV (curve c) compared to that obtained at the bare Pt electrode (curve a).

The enhancement of the ORR at the nano-MnOx/Pt electrodes is further verified by calculating the number of electrons (n) involved in the ORR as it is inherently related to the relative ratio of the disk and ring currents of the RRDE [Eq. (1),[21] in which $n=4$ if $I_R=0$ (i.e., no electrogeneration

$$n = 4-2\,I_R/N\,I_D \qquad (1)$$

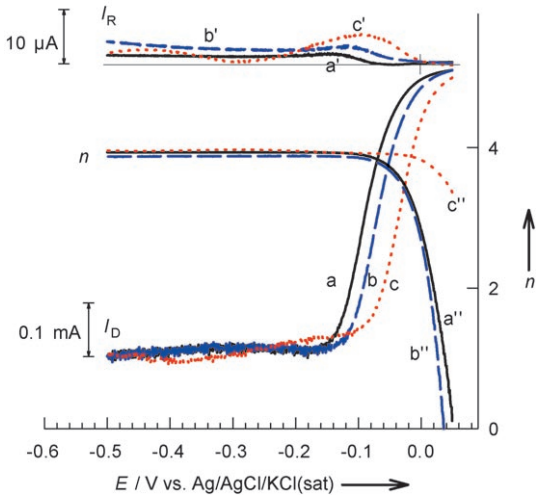

Figure 3. Steady-state voltammograms for the ORR, measured in O_2-saturated KOH (0.1 M), at a) bare Pt disk and b,c) nano-MnOx/Pt disk electrodes ($\phi=6.0$ mm). The electrodeposition conditions used for the MnOx preparation were the same as that described in the caption of Figure 1 with b) 5; c) 25 potential cycles. Rotation rate: 200 rpm; potential scan rate of the disk electrode: 10 mV s^{-1}. Curves a′–c′ represent the corresponding Pt-ring currents (polarized at +0.5 V). Curves a″–c″ represent the number of electrons (n) involved in the ORR at the different disk electrodes.

of hydrogen peroxide) and $n=2$ if the ratio $I_R/NI_D=1$ (i.e., exclusive reduction of oxygen to hydrogen peroxide), and N is the collection efficiency of the RRDE]. Curves a″–c″ of Figure 3 show the variation of n at the bare Pt (a″) and nano-MnOx/Pt disk electrodes (b″ and c″). Curve c″ demonstrates exclusive four-electron reduction of O_2 to water (or OH^- in alkaline medium) at the nano-MnOx/Pt electrode at a fairly positive potential compared with that at the bare Pt electrode (curve a″). The enhancement of the ORR in terms of a positive shift of the onset potential with a slight increase in the ring current (curve c′) may suggest a change in the reduction pathway of oxygen upon the electrodeposition of the MnOx nanoparticles onto the Pt surface.

To find out the origin of the ORR enhancement at the nano-MnOx/Pt electrodes, X-ray photoelectron spectroscopy (XPS) measurements of the electrodes were taken and the results are shown in Figure 4 A–C, in which the spectra of Pt 4f, Mn 2p, and O 1s orbitals are obtained at a) bare Pt and b,c) nano-MnOx/Pt surfaces. An inspection of Figure 4 reveals the following points: 1) Figure 4 A (curves a–c) shows that there is no significant change of the binding energies of the 4f orbitals of Pt upon loading MnOx nanoparticles. This fact indicates that the electronic structure of the Pt surface remains unchanged even after loading with nano-MnOx. Thus, the enhancement of the electrocatalytic performance after nano-MnOx loading does not originate from a change in the electronic properties of the Pt surface atoms. 2) Figure 4 B indicates that Mn exists in a cationic state rather than in an elemental state as evidenced from the positive shift of the 2p binding energy of Mn (a shift from 650 and 638.8 eV for $2p_{1/2}$ and $2p_{3/2}$ of elemental Mn to 653.8 and 641.7 eV, respectively, in the sample). 3) The XPS spectrum of the oxygen in MnOx (Figure 4 C) shows a rather broad peak

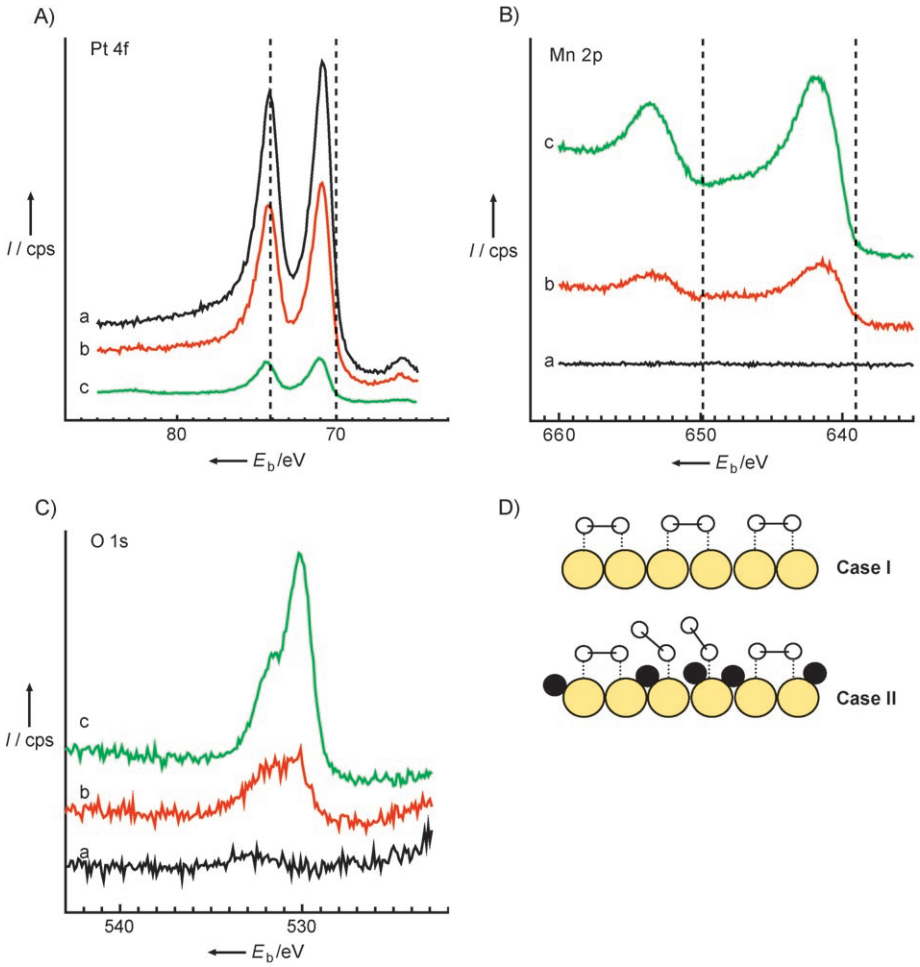

Figure 4. XPS spectra of A) Pt 4f, B) Mn 2p, and C) O 1s obtained for a) bare Pt and b,c) nano-MnOx/Pt electrodes. The electrodeposition conditions used for the MnOx preparation were the same as that described in the caption of Figure 1 with b) 25; c) 100 potential cycles. The dotted lines in Figures 4A and 4B correspond to the binding energies of $4f_{7/2}$ and $4f_{5/2}$ of elemental Pt and $2p_{1/2}$ and $2p_{3/2}$ of elemental Mn, respectively. D) Illustrates the proposed adsorption modes of molecular oxygen (small white circles) at the Pt surface (large yellow circles) in the absence (Case I) and presence (Case II) of nano-MnOx (black circles).

for the low loading of MnOx, which develops into a peak with a shoulder upon increasing the amount of the electrodeposited nano-MnOx (curve c). The origin of this split could be reasonably attributed to the presence of the oxygen in hydroxide and oxide forms in MnOOH.

As the catalytic reaction does not occur at any surface unless at least one of the reactants is chemisorbed, the observed enhancement of the electrocatalysis originates from a change in the adsorption orientation of molecular oxygen at the nano-MnOx/Pt surface. Figure 4D shows a diagram of the adsorption modes of molecular oxygen at bare Pt and nano-MnOx/Pt surfaces. At the bare Pt surface, the parallel adsorption orientation of O_2 molecules prevails (as evidenced from the almost-zero ring current in Figure 3, curve a′). Thus, the adsorption of one O_2 molecule per pair of Pt active sites is assumed. However, at the nano-MnOx/Pt surface, the adsorbed O_2 molecules have a mixed-orientation (i.e., parallel and end-on). The increased ring current provides evidence of end-on orientation, which reflects an increased amount of hydrogen peroxide present (as a two-electron reduction product; compare curves b′ and c′ with curve a′ of Figure 3). The mixed adsorption mode (Case II in Figure 4D) is assumed to result in the nano-MnOx/Pt surface having more adsorbed molecular oxygen species. In this case, the parallel and end-on orientation modes result in the adsorption of four oxygen molecules per three pairs of Pt active sites. Consequently, the higher degree of the adsorption of O_2 molecules in the latter case causes an increase in the pre-exponential factor of the Arrhenius equation for the ORR and thus a higher reaction rate is observed as a positive shift of the onset potential of the ORR. A similar explanation has been proposed by Paulus et al.[41] They found Arrhenius apparent activation energies for the ORR at different carbon-supported Pt–Ni and Pt–Co catalysts to be similar to that estimated at a carbon-supported Pt catalyst, although the former catalysts showed a higher catalytic activity than the latter. Thus, the pre-exponential factor in the Arrhenius rate expression has been assumed as the controlling parameter that determines the variations in the observed rates.[41]

In summary, the electrodeposition of manganese oxide nanorods onto Pt electrodes was found to cause a significant positive shift of the onset potential of the ORR compared with that at the bare Pt electrode. The change of the adsorption orientation of oxygen molecules, from the parallel (bridged) orientation at the bare Pt electrode to the mixed orientation of the parallel and end-on modes at the nano-MnOx/Pt electrode, is considered to be the cause for the higher population of oxygen molecules at the MnOx/Pt surface, which results in higher electrocatalysis for the ORR.

Received: February 22, 2006
Revised: June 14, 2006
Published online: August 4, 2006

Keywords: adsorption · electrochemistry · heterogeneous catalysis · nanostructures · surface chemistry

[1] "Development of non-platinum-based electrocatalysts for oxygen reduction": T. Ohsaka, M. S. El-Deab in *Recent Research Developments in Electrochemistry, Vol. 7*, Transworld Research Network Publisher, India, **2004**, and references therein.

[2] K. Kinoshita, *Electrochemical Oxygen Technology*, Wiley, New York, **1992**.
[3] N. M. Markovic, P. N. Ross, *Surf. Sci. Rep.* **2002**, *45*, 117, and references therein.
[4] C. H. Brian, A. Heinzel, *Nature* **2001**, *414*, 345.
[5] M. Watanabe, H. Igarashi, K. Yoshioka, *Electrochim. Acta* **1995**, *40*, 329.
[6] A. B. Anderson, J. Roques, S. Mukerjee, V. S. Murthi, N. M. Markovic, V. Stamenkovic, *J. Phys. Chem. B* **2005**, *109*, 1198, and references therein.
[7] T. J. Schmidt, U. A. Paulus, H. A. Gasteiger, R. J. Behm, *J. Electroanal. Chem.* **2001**, *508*, 41.
[8] N. M. Markovic, R. R. Adzic, B. D. Cahan, E. Yeager, *J. Electroanal. Chem.* **1994**, *377*, 249.
[9] M. T. Paffet, J. G. Beery, S. Gottesfeld, *J. Electrochem. Soc.* **1988**, *135*, 1431.
[10] F.-P. Hu, X.-G. Zhang, F. Xiao, J.-L. Zhang, *Carbon* **2005**, *43*, 2931.
[11] A. Bergel, D. Feron, A. Mollica, *Electrochem. Commun.* **2005**, *7*, 900.
[12] R. N. Singh, B. Lal, M. Malviya, *Electrochim. Acta* **2004**, *49*, 4605.
[13] H. Dafydd, D. A. Worsley, H. N. McMurray, *Corros. Sci.* **2005**, 47, 3006.
[14] O. S. -Feria, S. Duron, *Int. J. Hydrogen Energy* **2002**, *27*, 451.
[15] Y. Lin, X. Cui, X. Ye, *Electrochem. Commun.* **2005**, *7*, 267.
[16] M. Born, P. Bogdanoff, S. Fiechter, H. Tributsch, *J. Electroanal. Chem.* **2005**, *578*, 339.
[17] J. Hernandez, J. S. -Gullon, E. Herrero, *J. Electroanal. Chem.* **2004**, *574*, 185.
[18] J.-M. Leger, *Electrochim. Acta* **2005**, *50*, 3123.
[19] M. S. El-Deab, T. Ohsaka, *Electrochim. Acta* **2002**, *47*, 4255.
[20] M. S. El-Deab, T. Okajima, T. Ohsaka, *J. Electrochem. Soc.* **2003**, *150*, A851.
[21] M. S. El-Deab, T. Sotomura, T. Ohsaka, *Electrochem. Commun.* **2005**, *7*, 29.
[22] M. S. El-Deab, T. Sotomura, T. Ohsaka, *J. Electrochem. Soc.* **2005**, *152*, C1.
[23] F. Gao, M. S. El-Deab, T. Okajima, T. Ohsaka, *J. Electrochem. Soc.* **2005**, *152*, A1226.
[24] M. S. El-Deab, T. Sotomura, T. Ohsaka, *J. Electrochem. Soc.* **2005**, *152*, C730.
[25] Y. Zhang, S. Asahina, S. Yoshihara, T. Shirakashi, *Electrochim. Acta* **2003**, *48*, 741.
[26] K. Arihara, L. Mao, P. A. Liddell, E. M. -Ochoa, A. L. Moore, T. Imase, D. Zhang, T. Sotomura, T. Ohsaka, *J. Electrochem. Soc.* **2004**, *151*, A2047.
[27] L. Mao, K. Arihara, T. Sotomura, T. Ohsaka, *Electrochim. Acta* **2004**, *49*, 2515.
[28] L. Mao, D. Zhang, T Sotomura, K. Nakatsu, N. Koshiba, T. Ohsaka, *Electrochim. Acta* **2003**, *48*, 1015.
[29] M.-ki Min, J. Cho, H. Kim, *Electrochim. Acta* **2000**, *45*, 4211.
[30] T. Toda, H. Igarashi, M. Watanabe, *J. Electroanal. Chem.* **1999**, *460*, 258.
[31] T. Toda, H. Igarashi, M. Watanabe, *J. Electrochem. Soc.* **1998**, *145*, 4185.
[32] S. L. Brock, N. Duan, Z. R. Tian, O. Giraldo, H. Zhou, S. L. Suib, *Chem. Mater.* **1998**, *10*, 2619.
[33] J. Chen, J. C. Jin, V. Purohit, M. B. Cutlip, S. L. Suib, *Catal. Today* **1997**, *33*, 205.
[34] L. Mao, T. Sotomura, K. Nakatsu, N. Koshiba, D. Zhang, T. Ohsaka, *J. Electrochem. Soc.* **2002**, *149*, A504.
[35] T. Ohsaka, L. Mao, K. Arihara, T. Sotomura, *Electrochem. Commun.* **2004**, *6*, 273.
[36] M.-S. Wu, P.-C. J. Chiang, *Electrochem. Solid-State Lett.* **2004**, *7*, A123.
[37] E. Budevski, G. Staikov, W. J. Lorenz, *Electrochemical Phase Formation and Growth*, VCH, Weinheim, **1996**, chap. 4.
[38] Powder Diffraction File, W. F. McClune, Editor, International Center for Diffraction Data (ICDD), USA, **2003**.
[39] M. J. Garrido, *C. R. Hebd. Seances Acad. Sci.* **1935**, *200*, 69.
[40] E. Higuchi, H. Uchida, M. Watanabe, *J. Electroanal. Chem.* **2005**, *583*, 69.
[41] U. A. Paulus, A. Wokaun, G. G. Scherer, T. J. Schmidt, V. Stamenkovic, N. M. Markovic, P. N. Ross, *J. Phys. Chem. B* **2002**, *106*, 4181.

